Atmos. Chem. Phys. Discuss., doi:10.5194/acp-2016-381, 2016
Manuscript under review for journal Atmos. Chem. Phys.
Published: 9 June 2016

Atmospheric Chemistry and Physics Discussions

Regional and local variations in atmospheric aerosols using ground-based sun photometry during DRAGON in 2012

Itaru Sano[1], Sonoyo Mukai[2], Makiko Nakata[1], and Brent N. Holben[3]

[1]Kidai University, Higashi-Osaka, Japan
[2]The Kyoto College of Graduate Studies for Informatics, Kyoto, Japan
[3]NASA Goddard Space Flight Center, Greenbelt, MD, USA

Correspondence to: Itaru Sano (sano@info.kindai.ac.jp)

Abstract. The amount of long-range transboundary (LRT) aerosols over Japan is increasing due to growing anthropogenic emissions from the east Eurasian continent. This work investigates LRT aerosols based on a Distributed Regional Aerosol Gridded Observation Networks (DRAGON). We constructed DRAGON-Japan and -Osaka in spring of 2012. The former network covers almost all of Japan in order to obtain the contribution of LRT aerosols over Japanese islands. It was determined from the DRAGON-Japan campaign that the values of aerosol optical thickness (AOT) decrease from west to east during an aerosol episode. In fact, the highest AOT was recorded at Fukue Island in the western end of the network, and the value was much higher than that of urban areas. The latter network (DRAGON-Osaka) was set as a dense instrument network in the megalopolis of Osaka, with a population of 12 million, to better understand local emissions as well as the influence of LRT on urban areas.

AOT was further measured with a mobile sun photometer attached to a car. This transect information showed that aerosol concentrations rapidly changed in time and space together when most of the Osaka area was covered with moderate LRT aerosols. The combined use of the dense instrument network (DRAGON-Osaka) and high frequency measurements provides the motion of aerosol advection, which coincides with the wind vector around the layer between 700 and 850 hPa as provided by the reanalysis data of the National Centers for Environmental Prediction (NCEP).

1 Introduction

Aerosol data are important indications of the atmospheric environment. Aerosol controls the radiation balance by a light scattering and absorption process of incident solar radiation. Some types of aerosol indirectly contribute to the balance through the transformation of aerosols into cloud condensation nuclei (IPCC, 2013). The aerosols affect daily local air quality, i.e., visibility and concentrations of $\mathrm{PM}_{2.5}$ and PM_{10}. Villeneuve et al. (2015) have investigated the relationship between mortality and long-term exposure to $\mathrm{PM}_{2.5}$. They pointed out that long-term exposure of more than 11 $\mu\mathrm{g\,m}^{-3}$ of $\mathrm{PM}_{2.5}$ led to a definite increase in cardiovascular disease that increased mortality rates. The study was performed with a regional PM dataset derived from the Sea-viewing Wide Field-of-view Sensor (SeaWiFS), the Moderate Resolution Imaging Spectroradiometer (MODIS), and the Multi-angle Imaging Spectroradiometer (MISR) measurements and/or combination analyses of the Goddard Earth Observing System (GEOS)-Chem chemical transport model and satellite results (van Donkelaar et al., 2015). Estimations

Atmos. Chem. Phys. Discuss., doi:10.5194/acp-2016-381, 2016
Manuscript under review for journal Atmos. Chem. Phys.
Published: 9 June 2016

Atmospheric Chemistry and Physics Discussions

of $PM_{2.5}$ based on satellite data require accurate derivations of the vertical profile of aerosol optical thickness (AOT) with fine spatial resolution. Nevertheless, current algorithms for space-based aerosol retrieval are not suitable to resolve this issue because they are tuned for analysis on a global scale, and they sometimes result in a large number of uncertainties for not only a very bright target but also for a complex mixture such as an urban area.

In the early 1990s, the Aerosol Robotic Network (AERONET) (Holben et al., 1998) was established to support the validation of aerosol products by NASA's EOS-MODIS (Terra) and MODIS (Aqua) missions (King et al., 1992). The AERONET program measures AOT from UV to near infrared with high accuracy. It also provides the optical and microphysical properties of aerosols (Dubovik and King, 2000). Dubovik et al. (2002) provided a climatology dataset of global aerosol characteristics, and the categorized results of the characteristics are presented by Omar et al. (2005). The compiled results of aerosol information are useful for the preparation of a look-up table on aerosol retrieval procedures from satellite measurements. There are currently around 400 sites collecting aerosol measurements around the world. However, most of the AERONET site is representative of a targeted area. This deployment style would not provide sufficient measurements for future aerosol retrieval algorithms (Kokhanovsky et al., 2015), such as extracting aerosol properties with fine resolution or vertical distribution, and considering a mixture of ground conditions. In order to apply these requirements, the AERONET group has embarked on a special campaign to deploy many AERONET instruments in a specific area, which is called a distributed regional aerosol gridded observation networks (DRAGON). The DRAGON style measurements contribute not only to developing and validating satellite aerosol retrieval algorithms but also to validating the aerosol transport simulation, e.g., the GEOS-Chem (Bey et al., 2001; Martin et al., 2003), the Weather Research and Forecasting WRF-Chem (Grell et al., 2005) and Spectral Radiation-Transport Model for Aerosol Species (SPRINTARS) (Takemura et al., 2015).

The first DRAGON was created in the Washington, D.C.-Baltimore region in 2011 (Holben et al., 2010). In spring of 2012, DRAGON-Japan and -Korea were formed. This work describes the behavior of transboundary aerosol properties based on two kinds of ground measurements in a large gridded network (DRAGON-Japan) and a small one (DRAGON-Osaka).

2 DRAGON-Japan

2.1 Background of DRAGON-Japan

The solid line in Fig. 1 shows the monthly average values of AOT at a wavelength of 500 nm over the AERONET Osaka site. The highest average AOT is around $\sim$0.4 in May and a lower value of $\sim$0.2 is recorded in winter. The dashed line represents the wavelength tendency (Ångström exponent (AE)) of two AOT values in log-scale. Wavelengths of 440 and 870 nm were taken as the AERONET standard. AE is an index of the size of particles. Small particles, e.g., carbonaceous, sulfuric, and other anthropogenic particles, have high AEs (Eck et al., 1999). A low AE denotes coarse particles such as desert dust or sea salt (Sano et al., 2003). It is evident from Fig. 1 that the AE has a lower value in spring and a higher value in summer or winter. In spring in East Asia, large desert dust particles are frequently observed from February to May. The Asian dust events result in a lower AE. At the same time, dust events bring a larger amount of particles with a high AOT. Such turbid conditions continue until August even after the Asian dust season has ended. On the other hand, AE increases rapidly from May to July,

Atmos. Chem. Phys. Discuss., doi:10.5194/acp-2016-381, 2016
Manuscript under review for journal Atmos. Chem. Phys.
Published: 9 June 2016

Atmospheric Chemistry and Physics Discussions

and then drops in August. With respect to aerosols in summertime, we assume the following three conditions: a high oxidant (O_x) level from local and transboundary emissions, high temperature, and strong solar incident light, which may affect the increase in the conversion process of secondary organic aerosols (SOAs) from volatile organic compounds (VOCs) through the photochemical process (Matsumoto, 2014). SOAs are also known as $PM_{2.5}$ particles (Hara et al., 2011), which have a high AE. In fact, high values of O_x are recorded at many environmental monitoring stations (AEROS , http://soramame.taiki.go.jp/). Thus, high values of AOT and AE are realized in Japanese summers. It is possible that spring is the best season to investigate the contribution from China of long-range transboundary (LRT) aerosols over Japan.

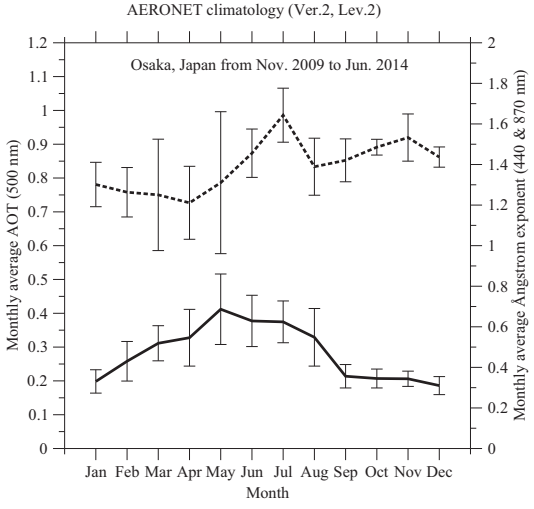

Figure 1. Solid and dashed lines represent monthly average aerosol optical thickness (AOT) at 500 nm and Ångström exponent (440 and 870 nm) over the AERONET Osaka (34.6° N, 135.6° E) station in Japan from November 2009 to June 2014, respectively. Error bars represent the standard deviation.

2.2 Observations during DRAGON-Japan

Figure 2 represents the instrument setting during DRAGON-Japan. As mentioned above, the objective of DRAGON-Japan is to investigate LRT aerosols from the Asian continent. Thus, most instruments are set from the western to the middle region of Japan. The National Institute of Environmental Studies (NIES) has been operating the Asian Dust and aerosol lidar observation Network (AD-Net) LIDAR in Fukue Island, Fukuoka, Matsue, Osaka, and Tsukuba to monitor the dust transportation (Sugimoto et al., 2003; Sano et al., 2008; Shimizu et al., 2015). Thus, the DRAGON-Japan instruments were co-located near the position of AD-Net LIDAR. In Fig. 2, open circles indicate the positions of both AERONET and LIDAR instruments during the DRAGON period. The LIDAR gives attenuated backscatter coefficients of 532 and 1064 nm as well as a depolarization ratio at 532 nm channel. Shimizu et al. (2004) successfully delineated two components of the extinction profile as sphere and non-sphere (dust aerosols) using the LIDAR measurements. In addition, filled circles in Fig. 2 represent the deployment of an AERONET instrument alone.

Atmos. Chem. Phys. Discuss., doi:10.5194/acp-2016-381, 2016
Manuscript under review for journal Atmos. Chem. Phys.
Published: 9 June 2016

Atmospheric Chemistry and Physics Discussions

Figure 3 shows average AOT at 500 nm during DRAGON-Japan. The results from Matsue have been discarded because there were an insufficient number of measurements compared to other locations due to system problems with the satellite transmitter during the period. In addition, results from Chiba and Kohriyama were also eliminated because average AOT values were similar to Tsukuba. It is easily understood from Fig. 3 that the AOT values decrease with longitude. In other words, western Japan exhibits higher AOT than eastern Japan.

The maximum average AOT was recorded in Fukue Island, which is located in the East China Sea (see Fig. 2). Also, the variation of AOT at Fukue is larger than at the other sites. The local emissions would seem to be small on Fukue Island due to a population of only 37,000. Moreover, the measurements were taken at the Fukue aerosol observatory on the peninsula northwest of the island, which is far from the center of town. Therefore, it is natural to consider that the large values of AOT at Fukue represent the dense LRT haze over the entire island. Fukuoka is a million city and strongly affected by transported aerosols. This fact is also seen in the sites of Nishi-harima and Noto, which are located far from large cities in Japan. It might be caused by the influence of LRT aerosols over the Sea of Japan. Even those locations exhibit values of AOT similar to Tsukuba, where the AOT level is most likely affected by emissions from the Tokyo area. It is clear in Fig. 3 that the AOT value at Osaka is rather high compared to the AOT trend with longitude. The Osaka megalopolis emits huge amounts of air pollution, and hence the AOT has a higher value due to the mixture of local emissions with LRT aerosols, which is explored in more depth in the following section.

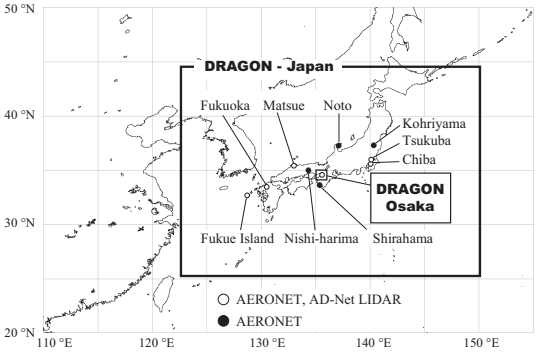

Figure 2. Geographical positions of observational sites for DRAGON-Japan in spring of 2012.

3 DRAGON-Osaka

3.1 Observations during DRAGON-Osaka

Figure 4 shows an enlarged area of DRAGON-Osaka, as shown in Fig. 2. A small gridded AERONET sun/sky radiometer network was set from March to May of 2012 in the Osaka metropolitan area. It involved Kobe, Kyoto, Nara, and other cities, and the region is the second largest populated area in Japan, with a population of 12 million people (see Fig. 4). Aerosol retrieval over this region from a satellite is difficult, although the AERONET sun/sky radiometer has been set since autumn

Atmos. Chem. Phys. Discuss., doi:10.5194/acp-2016-381, 2016
Manuscript under review for journal Atmos. Chem. Phys.
Published: 9 June 2016

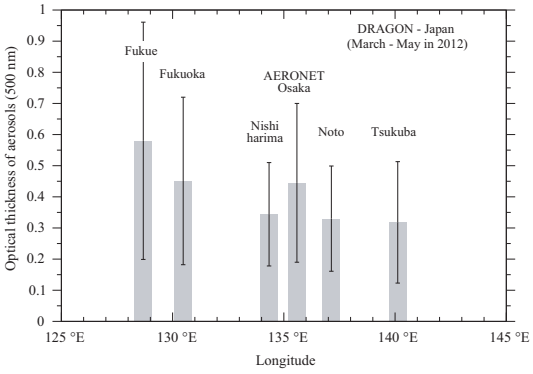

Figure 3. Average AOT at a wavelength of 500 nm during the DRAGON-Japan period. Measurements were taken at Fukue Island, Fukuoka, Nishi-harima, Osaka, Noto, and Tsukuba (see Fig. 2). The error bars represent standard deviation at each site.

2001. In fact, MODIS level 2 aerosol products (MxD04s) sometimes do not provide us with aerosol information from this area. This might be due to such issues as too bright a target, a complex mixture of ground conditions, validation data from only a specific place (AERONET Osaka site), and so on. The first issue occurs by miss reorganization as a cloudy area. The second issue is a more difficult problem. Land use in a Japanese urban area is very complicated. Because most of Japan (80%) is mountainous, a majority of the population lives in flat areas. Thus, a pixel of a satellite image may include many types of structures and various ground conditions.

DRAGON-Osaka intends to provide local aerosol conditions for an algorithm development of satellite data and an aerosol transport model (Sano et al., 2012). A better understanding of local variations in aerosol properties is important for precise ground modeling. Therefore, the DRAGON-Osaka project constructed a more dense sun/sky radiometer network compared to other DRAGON projects. The AERONET Osaka site in Fig. 4 is a steady site. Other sites (open circles) are temporary sites during the DRAGON-Osaka campaign. Seven AERONET instruments were deployed in flat locations in the Osaka region ([AERONET-]Osaka, Kobe, Osaka-N[orth], Osaka-C[enter], Osaka-S[outh], Kyoto, and Nara; characters in square brackets will be omitted hereinafter). Two mountain sites were set in Mt. Rokko and Mt. Ikoma, at around 790 m and 640 m above sea level (ASL), respectively. The Kobe (Kobe Univ.) site faces Osaka Bay, Osaka-N (Kansai Univ.) is surrounded by a residential area, and Osaka-C (Kimoto Electric Co.) is nearest to downtown Osaka. The AERONET Osaka (Kindai Univ.) site is located in eastern Osaka close to Mt. Ikoma. Mt. Ikoma is the boundary between Osaka and Nara prefectures. The Osaka-S (Osaka Pref. Univ.) site is in the urban area and is close to large industrial oil plants. The Kyoto site (Kyoto Univ.) is located near the mountain, yet is close to a busy section of Kyoto. The Nara site (Nara Women Univ.) is in the center of Nara.

Figure 5 represents the daily average values at each site on April 24 (denoted by filled circles), April 27 (open circles), and average values (squares) during DRAGON-Osaka. The measurements are carefully selected from AERONET Version 2 Level 2 by checking all sky images, which were taken every 2 min at the AERONET Osaka site. Some measurements are also added by checking the images from Level 1 data. Each error bars show the standard deviation of the daily variation.

Atmos. Chem. Phys. Discuss., doi:10.5194/acp-2016-381, 2016
Manuscript under review for journal Atmos. Chem. Phys.
Published: 9 June 2016

Atmospheric Chemistry and Physics Discussions

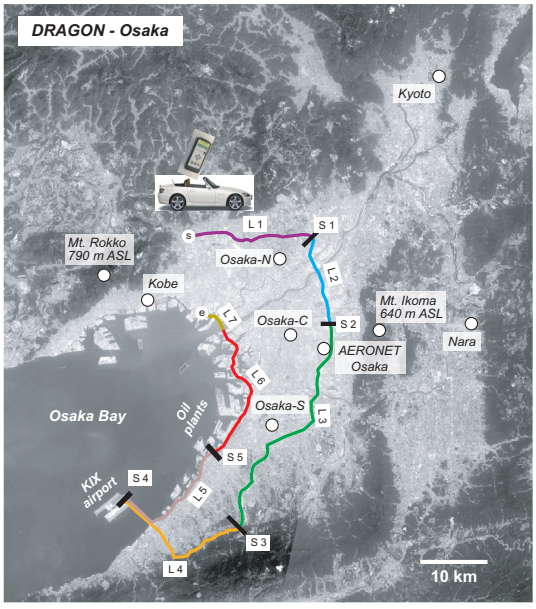

Figure 4. Site deployment during DRAGON-Osaka in spring 2012. Colored lines indicate the path of transect measurements.

On April 27, all DRAGON-Osaka sites showed the lowest values of AOT. This means that the 27th was the clearest day during the period. Also, it was a Friday, which was a usual business day before the beginning of a short vacation period in Japan from the end of April to the beginning of May. Thus, the values may contain a substantial amount of information on local emissions. The order of AOT from highest to lowest is as follows: Osaka (∼0.15), Osaka-C (∼0.14), Osaka-S (∼0.14), Osaka-N (∼0.12), Kobe (∼0.12), and Kyoto (∼0.12). Note that the Nara site had a value of around 0.10, but the number of measurements from the site were insufficient for discussion. Figure 5 presents the acceptable results because Osaka and Osaka-C sites are located in busy areas and are just 5.8 km from each other. Osaka-S is close to large industries and thus has a high value.

On April 24, every site recorded the highest AOT values during the period. It seems that the entire Osaka area was covered with a dense aerosol concentration. For example, Kyoto had an AOT of ∼1.0. Thus, a large amount of LRT aerosols were superposed over the local emissions.

The average values are also presented by squares in Fig. 5. A list of AOT from highest to lowest is as follows: Osaka (∼0.40), Osaka-C (∼0.39), Kobe (∼0.38), Osaka-S (∼0.38), Osaka-N (∼0.37), and Kyoto (∼0.35). This result is similar to that in a clear day. Thus, the measurements on the 27th represent the intrinsic local emissions of aerosols.

3.2 Transect measurements

The transect measurements of AOT were taken on May 5, 2012, during a short Japanese vacation season, and, thus, a period of low industrial activity. Accordingly, our experimental results are expected to show LRT aerosols rather than local emissions.

Atmos. Chem. Phys. Discuss., doi:10.5194/acp-2016-381, 2016
Manuscript under review for journal Atmos. Chem. Phys.
Published: 9 June 2016

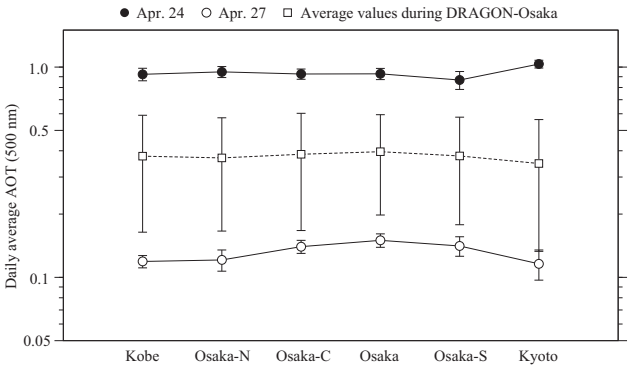

Figure 5. Comparison of daily average values of AOT (500 nm) at each site on April 24 (hazy day) and April 27 (clear day), denoted by the filled and open circles, respectively. The average values over the DRAGON period are denoted by squares.

The authors attempted to measure the spatial variation of AOT measurements using a combination of a mobile sun photometer (Microtops-II (MT-2)) and a convertible car. The observed wavelengths of AOT measurements by MT-2 were the same as the AERONET instrument at 380, 440, 500, 670, and 870 nm. Note that the calibration of MT-2 was performed in February 2012 at NASA/GSFC according to the maritime aerosol network (MAN) procedure (Smirnov et al., 2009). A difficulty of on-board measurements is targeting direct sunlight due to the movement of the car. In order to avoid contaminating noise, two rules were employed: standard deviation of signals, which is automatically recorded by MT-2, should take a small value, and the variation of AE during a few minutes should also be small.

The AOT transect was obtained along the highway, as shown by several colors in Fig. 4, which is divided into seven different colored legs along the roads and five stops labeled L1 to L7 and S1 to S5, respectively. The measurements of the stopping points (S1-S5) were taken at each location where the car was parked, and where a highly accurate AOT was obtained because of the car being still. The car was maintained at a speed of around 70-90 $\mathrm{km\,h^{-1}}$ in order to obtain accurate AOT measurements. The obtained AOT (500 nm) values are presented in Fig. 6. The measurements in each leg are shown by the same color circles as used in Fig. 4 and black filled circles indicate the measurements at stopping points S1-S5.

The car began at 9:20 (local time) from starting point L1 (northwest in the Osaka area), then traveled east and passed close to the Osaka-N site. The magnitude of AOT (500 nm) gradually increased from ∼0.37 to ∼0.43 during the first 20 min. Then the car changed direction and traveled south (L2). At L2 the AOT gradually decreased from ∼0.43 to ∼0.38. The car passed through the nearest location of the Osaka site in L3. A comparison of AOT by MT-2 with DRAGON-Osaka was performed when the distance between the car and the site was within 1.5 km. The AOT values from MT-2 were 0.406 at 10:15:21 and 0.399 at 10:15:31 local time. The value of the Osaka site measurement taken nearest to the time of the car measurements was 0.400 at 10:18:57. The transect measurements during L3 coincided with the products observed at the corresponding Osaka site. This demonstrates that our MT-2 measurements can be utilized to understand the aerosol condition of the Osaka urban area.

AOT gradually decreased along L4 and finally increased near the car stopping point (S4) at Kansai International Airport (KIX). We recorded AOT values for one hour with no car movement at KIX. The time series trend is nearly stable but we see

Atmos. Chem. Phys. Discuss., doi:10.5194/acp-2016-381, 2016
Manuscript under review for journal Atmos. Chem. Phys.
Published: 9 June 2016

Atmospheric Chemistry and Physics Discussions

gentle decreases during the period. On-board AOT values were low and stable in L5, the same as at KIX. After the final stop of S5, MT-2's internal memory was full, so the number of measurements was limited in L6 and L7. However, we successfully measured an increase in AOT values from ∼0.35 to ∼0.46 in L6 and a decrease to ∼0.33 in L7. This might be due to dense aerosol that covers only a small region just over the highway.

At the same time the transect measurements are taken, the minute placement of AERONET instruments also must present detailed aerosol information. Figure 7 shows AOT measurements that were observed by the DRAGON-Osaka network. The measurements of Osaka-C, Osaka, and Osaka-S are plotted as thin dotted, thin solid, and thin dashed lines, respectively. Filled squares and open squares represent the values of AOT that were taken at Kobe and Osaka-N sites. Continuous measurements of Osaka-C, Osaka, and Osaka-S were measured by the AERONET sun photometer in high frequency measurement mode, or the O'Neill mode (or turbo mode in the recent new control box). Measurements were taken in approximately three minute intervals. However, Kobe and Osaka-N sites did not employ this continuous measurement scheme because of a different data acquisition system. Comparing Fig. 7 with Fig. 6 with respect to the Osaka site, AOT variations from both the AERONET site and MT-2 coincided, especially AOT peaks around 10:30-11:30 and 13:00-14:00. This will be discussed further in section 4. In addition, the first AOT peak from L1 (purple) to L2 (blue) periods might be the aerosol plume that passed around 9:20 at the Osaka-N site.

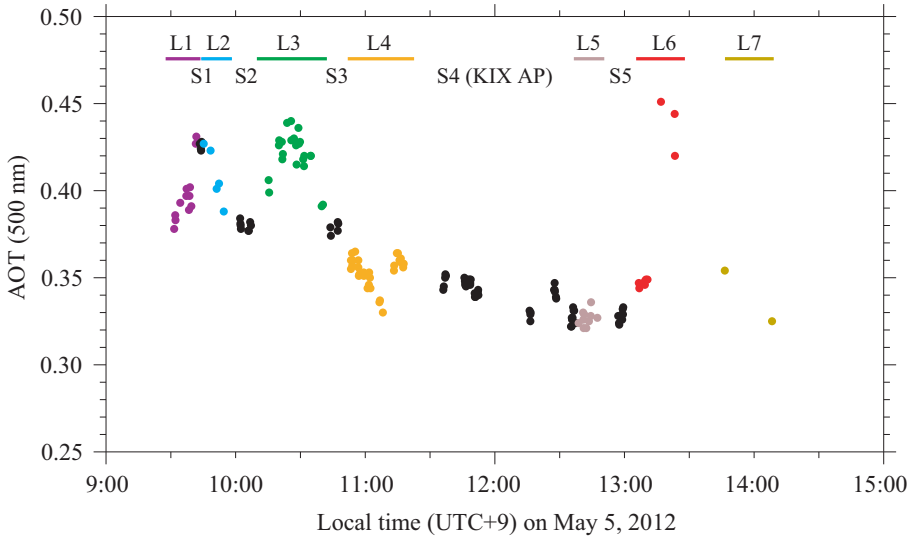

Figure 6. The values of AOT (500 nm) measured with Microtops-II by car on May 5. Each color of the filled circles represents the corresponding color of the transect path in Fig. 4. The black filled circles indicate the measurements of AOT at the stopping points, S1 to S5.

Atmos. Chem. Phys. Discuss., doi:10.5194/acp-2016-381, 2016
Manuscript under review for journal Atmos. Chem. Phys.
Published: 9 June 2016

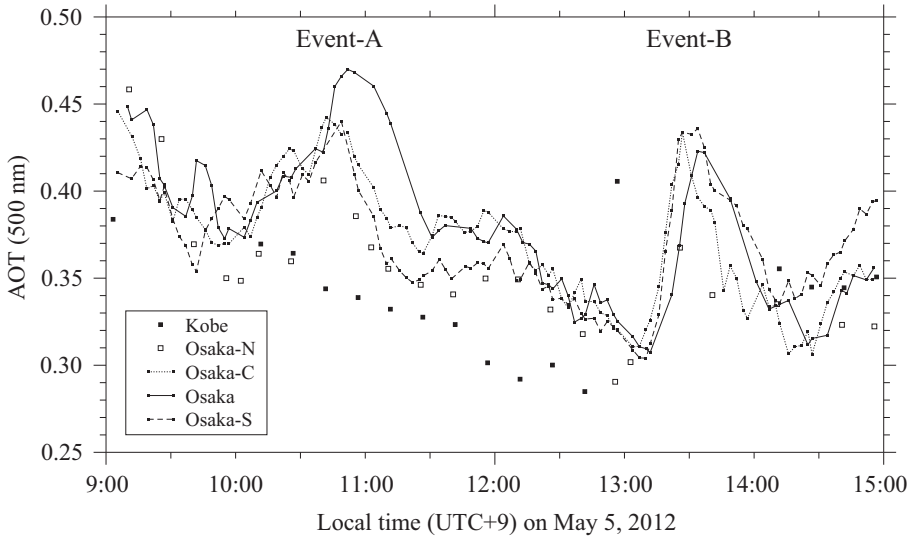

Figure 7. AOT (500 nm) measurements observed by DRAGON-Osaka sites on May 5, 2012.

4 Discussion and conclusions

Two large AOT peaks, as seen in Fig. 7, were observed from 10:30-11:30 (called event-A hereinafter) and around 13:00-14:00 (event-B), respectively. Both events-A and -B during DRAGON-Osaka are good representatives of air mass advection because the values of AOT were higher at all sites than the monthly average AOT at the AERONET Osaka site (see Fig. 1). Further, during events-A and -B, AOT showed similar time variations at every location involved in the DRAGON-Osaka project.

Event-A started a few minutes after 10:00 at all sites, and continued until 11:00 (see Fig. 7). It is noted that the Osaka site has shown different behaviors from other sites; for example, there were explicitly higher values and longer periods of high values than those at Osaka-C and Osaka-S sites. To understand this difference in behavior, the collocated AD-Net LIDAR system at Osaka site is available. The LIDAR system provided us with the vertical distribution of aerosols. Figures 8a and 8b show the time series of the attenuated backscatter ratio and depolarization ratio, respectively, at a wavelength of 532 nm. It is found from Fig. 8a that the ratio suddenly increased from a lower to a higher altitude just before a local time of 9:00 (UTC+9), and high aerosol concentrations were composed of two layers, a lower (<500 m) and a higher one (>500 m). The high concentration in the lower layer below 500 m continued during the entire day, but the altitude of the higher layer dramatically changed in temporal scale. Namely, the variability of high altitude AOT is larger than that of low layer AOT in the case of event-A. The minimum value of AOT during the day seems to be around 0.3 according to Fig. 7. If we assume that this value is constantly provided from a low layer (<500m), the change of total AOT could be due to a change in high altitude aerosols alone, where the value is around a maximum of 0.15 during event-A (see Fig. 7).

In respect to event-B, a similar trend of rapid increasing and decreasing of AOT at all sites was found. It is noted that the up and down timing of AOT was synchronized at Osaka-C, Osaka-S, and the Osaka site, but event-B was slightly delayed

Atmos. Chem. Phys. Discuss., doi:10.5194/acp-2016-381, 2016
Manuscript under review for journal Atmos. Chem. Phys.
Published: 9 June 2016

Atmospheric Chemistry and Physics Discussions

at the Osaka site. Shinozuka and Redemann (2011) have pointed out that LRT aerosols retain their concentrations more than local emissions even after long-range transport based on auto correlated analysis. It is possible to say that these measurements indicate the transition of air parcel involving a dense concentration of aerosols. This fact coincided with measurements of depolarization ratio in Fig. 8b, which suggests us the existence of LRT dust concentration at that time.

It is of interest that the behavior of AOT at the Osaka site differs slightly from that at the Osaka-C and -S sites during both events-A and -B. From the geographic map in Fig. 4, it is seen that the Osaka site is located in the eastward direction from the Osaka-C and -S sites. The straight distance between Osaka-C and Osaka site is 5.8 (∼6) km. An AOT value of 0.3450 was recorded at 13:15:56 (local time) at the Osaka-C site. Six minutes later, the Osaka site provided 0.3464 of AOT at 13:21:56. Therefore, it took 6 min to travel from west to east at a rate of 16 $\mathrm{m\,s^{-1}}$. This assumption coincides with the reanalysis data by NCEP (Kalnay et al., 1996). Figure 9 shows the wind vector information over Japan at the 700 hPa-level at 15:00 local time (6:00 UTC) on May 5, 2012, by NCEP. The wind direction and speed were eastward and around 16-18 $\mathrm{m\,s^{-1}}$ over the area.

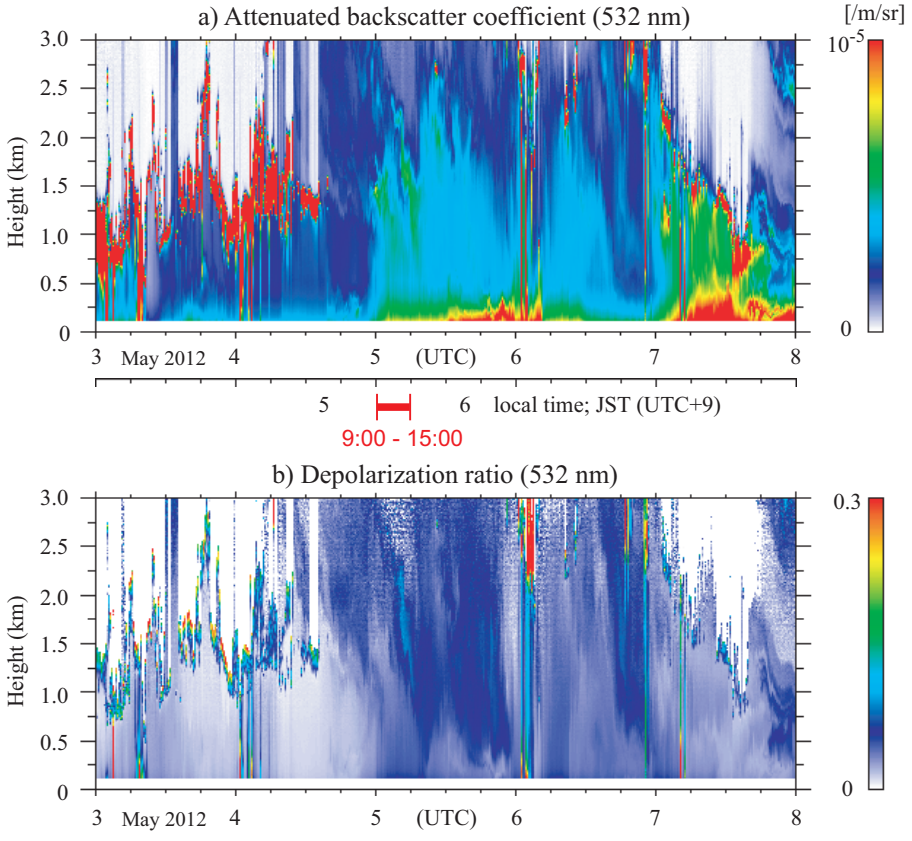

Figure 8. a) Attenuated backscatter coefficient at 532 nm by AD-Net LIDAR at the AERONET-Osaka site from May 3 to May 5; b) depolarization ratio at 532 nm. Red bar corresponds to the observation period of Figs. 6 and 7.

Atmos. Chem. Phys. Discuss., doi:10.5194/acp-2016-381, 2016
Manuscript under review for journal Atmos. Chem. Phys.
Published: 9 June 2016

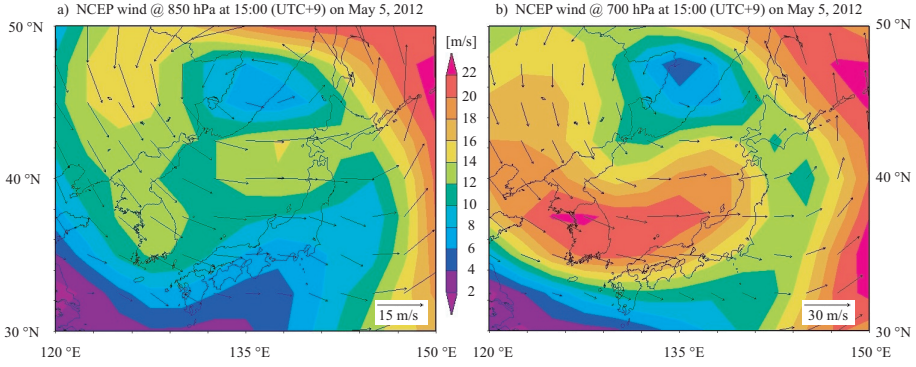

Figure 9. a) Wind direction and speed at the 850 hPa level over Japan at 15:00 local time (UTC+9) on May 5, 2012, by NCEP; b) Wind direction and speed at the 700 hPa level over Japan at 15:00 local time (UTC+9) on May 5, 2012, by NCEP.

The variation in atmospheric aerosols on a regional and areal scale based on DRAGON-Japan and -Osaka experiments has been investigated in this work and the following conclusions have been drawn:

1. High AOT in western Japan measured in the spring of 2012 decreased with longitude. This suggests that long-range transported aerosols from the continent affect the atmospheric condition even in remote areas of Japan.

2. The AOT values along the Sea of Japan were high and equaled the values in the suburbs of Tokyo. It might be expected that aerosol was transported over the Sea of Japan.

3. A dense instrument network reveals the magnitude and distribution of local emissions in Osaka, which suggests that the average AOT was around 0.15 and variations of the values are ∼0.03 during the observation period.

4. Both transect and DRAGON-Osaka measurements indicate that the distribution of aerosol concentrations is not homogeneous even after transportation over a few thousand km. This suggests that ground remote sensing measurements should be taken more frequently (like the turbo or O'Neill mode in AERONET) and satellite measurements should be provided at a more fine resolution for comparison with the ground-based measurements.

5. The DRAGON-style gridded deployment and high frequency measurements provide not only information on local aerosols but on long transportation. For example, it was found from DRAGON-Osaka that the transportation speed of the upper aerosol layer coincides with NCEP wind speed.

Acknowledgements. First, the authors are grateful to all collaborators in DRAGON-Japan, and acknowledge NASA for the AERONET team and NIES/LIDAR group for data processing. This work was supported in part by the Global Change Observation Mission-Climate 1st (GCOM-C1) project by JAXA (no. JX-PSPC-308878). This study was supported in part by the Global Environment Research Fund of the Ministry of Environment, Japan (S-12) and JSPS KAKENHI Grant Numbers 25340019 and 15K00528.

Atmos. Chem. Phys. Discuss., doi:10.5194/acp-2016-381, 2016
Manuscript under review for journal Atmos. Chem. Phys.
Published: 9 June 2016

Atmospheric Chemistry and Physics Discussions

References

AEROS, Atmospheric Environmental Regional Observation System, http://soramame.taiki.go.jp/ (accessed on March 10, 2016).

Bey, I., Jacob,D.J., Yantosca, R.M., Logan, J.A., Field, B.D., Fiore, A.M., Li, Q., Liu, H.Y., Mickley, L.J., and Schultz, M.G.: Global modeling of tropospheric chemistry with assimilated meteorology: Model description and evaluation, J. Geophys. Res., 106, 23073–23095, doi:10.1029/2001JD000807, 2001.

Dubovik, O., and King, M.D.: A flexible inversion algorithm for retrieval of aerosol optical properties from sun and sky radiance measurements, J. Geophys. Res., 105, 20673–20696, doi:10.1029/2000JD900282, 2000.

Dubovik, O., Holben, B.N., Eck, T.F., Smirnov, A., Kaufman, Y.J., King, M.D., Tanré, D. and Slutsker, I.: Variability of absorption and optical properties of key aerosol types observed in worldwide locations, J. Atmos. Sci., 59, 590–608, doi:10.1175/1520-0469(2002)059<0590:VOAAOP>2.0.CO;2, 2002.

Eck, T.F., Holben, B.N., Reid, J.S., Dubovik, O., Smirnov, A., O'Neill, N.T., Slutsker, I., and Kinne, S.: Wavelength dependence of the optical depth of biomass burning, urban, and desert dust aerosols, J. Geophys. Res., 104, D24, 31333–31349, doi:10.1029/1999JD900923, 1999.

Grell G.A., Peckham, S.E., Schmitz, R., McKeen, S.A., Frost, G., Skamarock, W.C., and Eder, B.: Fully coupled "online" chemistry within the WRF model, Atmos. Environ., 39, 6957–6975, doi:10.1016/j.atmosenv.2005.04.027, 2005.

Hara, Y., Uno, I., Shimizu, A., Sugimoto, N., Matsui, I., Yumimoto, K., Kurokawa, J., Ohara, T., and Liu, Z.: Seasonal characteristics of spherical aerosol distribution in eastern Asia: Integrated analysis using ground/space-based lidars and a chemical transport model, SOLA, 7, 121–124, doi:10.2151/sola.2011-031, 2011.

Holben, B.N., Eck, T.F., Slutsker, I., Tanré, D., Buis, J.P., Setzer, A., Vermote, E., Reagan, J.A., Kaufman, Y.J., Nakajima, T., Lavenu, F., Jankowiak, I., and Smirnov, A.: AERONET–A federated instrument network and data archive for aerosol characterization, Rem. Sens. Environ., 66, 1–16, doi:10.1016/S0034-4257(98)00031-5, 1998.

Holben, B.N., Eck, T., Schafer, J., Giles, D., and Sorokin M.: Distributed Regional Aerosol Gridded Observation Networks (DRAGON) White Paper, 2010, http://aeronet.gsfc.nasa.gov/new_web/Documents/DRAGON_White_Paper_A_system_of_experiment.pdf (accessed on March 10, 2016).

IPCC, Climate Change 2013: The Physical Science Basis. Contribution of Working Group I to the Fifth Assessment Report of the Intergovernmental Panel on Climate Change [Stocker, T.F., Qin, D., Plattner, G.-K., Tignor, M., Allen, S.K., Boschung, J., Nauels, A., Xia, Y., Bex, V., and Midgley, P.M. (eds.)], Cambridge University Press, Cambridge, UK, and New York, USA, 2013.

Kalnay, E., Kanamitsu, M., Kistler, R., Collins, W., Deaven, D., Gandin, L., Iredell, M., Saha, S., White, G., Woollen, J., Zhu, Y., Leetmaa, A., Reynolds, R., Chelliah, M., Ebisuzaki, W., Higgins, W., Janowiak, J., Mo, K. C., Ropelewski, C., Wang, J., Jenne, R., and Joseph, D.: The NCEP/NCAR 40-year reanalysis project, Bull. Amer. Meteor. Soc., 77, 437–470, doi:10.1175/1520-0477(1996)077<0437:TNYRP>2.0.CO;2, 1996.

King, M.D., Kaufman, Y.J., Menzel, W.P., and Tanré, D.: Remote sensing of cloud, aerosol, and water vapor properties from the Moderate Resolution Imaging Spectrometer (MODIS), IEEE Trans. Geosci. Remote Sensing, 30, 1, 2–27, doi:10.1109/36.124212, 1992.

Kokhanovsky, A.A., Davis, A.B., Cairns, B., Dubovik, O., Hasekamp, O.P., Sano, I., Mukai, S., Rozanov, V.V., Litvinov, P., Lapyonok, T., Kolomiets, I.S., Oberemok, Y.A., Savenkov, S., Martin, W., Wasilewski, A., Di Noia, A., Stap, F.A., Rietjens, J., Xu, F., Natraj, V., Duan, M., Cheng, T., and Munro, R.: Space-based remote sensing of atmospheric aerosols: The multi-angle spectro-polarimetric frontier, Earth - Science Reviews, 145, 85-116, doi:10.1016/j.earscirev.2015.01.012, 2015.

Atmos. Chem. Phys. Discuss., doi:10.5194/acp-2016-381, 2016
Manuscript under review for journal Atmos. Chem. Phys.
Published: 9 June 2016

Martin, R.V., Jacob, D.J., Yantosca, R.M., Chin, M., and Ginoux, P.: Global and regional decreases in tropospheric oxidants from photochemical effects of aerosols, J. Geophys. Res., 108, 4097, doi:10.1029/2002JD002622, 2003.

Matsumoto, J.: Measurements of total radical reactivity of volatile organic compounds (VOCs) and total organic nitrates to evaluate secondary organic aerosol (SOA) formation (in Japanese), Earozoru Kenkyu, 29, 47–54, doi:10.11203/jar.29.s47, 2014.

Omar, A.H., Won, J.-G., Winker, D.M., Yoon, S.-C., Dubovik, O., and McCormick, M.P.: Development of global aerosol models using cluster analysis of Aerosol Robotic Network (AERONET) measurements, J. Geophys. Res., 110, D10, D10S14, doi:10.1029/2004JD004874, 2005.

Sano, I., Mukai, M., Okada, Y., Mukai. S., Sugimoto, N., Matsui, I., and Shimizu, A.: Improvement of PM2.5 analysis by using AOT and lidar data, Proc. SPIE 7152, Remote Sensing of the Atmosphere and Clouds II, 71520M (December 08, 2008), doi:10.1117/12.804903, 2008

Sano, I., Mukai, S., Holben, B.N., Nakata, M., Yonemitsu, M., Sugimoto, N., Fujito, T., Hiraki, T., Iguchi, N., Kozai, K., Kuji, M., Muramatsu, K., Okada, Y., Okada, Y., Sadanaga, Y., Tohno, S., Toyazaki, Y., and Yamamoto, K.: DRAGON-West Japan campaign in 2012: Regional aerosol measurements over Osaka, Proc. SPIE 8523, Remote Sensing of the Atmosphere, Clouds, and Precipitation IV, 85231M (Nov. 8, 2012), doi:10.1117/12.977615, 2012.

Sano, I., Mukai, S., Okada, Y., Holben, B.N., Ohta, S., and Takamura, T.: Optical properties of aerosols during APEX and ACE-Asia experiments, J. Geophys. Res., 108, 8649, doi:10.1029/2002JD003263, 2003.

Shimizu, A., Sugimoto, N., Matsui, I., Arao, K., Uno, I., Murayama, T., Kagawa, N., Aoki, K., Uchiyama, A., and Yamazaki, A.: Continuous observations of Asian dust and other aerosols by polarization lidars in China and Japan during ACE-Asia, J. Geophys. Res., 109, D19S17, doi:10.1029/2002JD003253, 2004.

Shimizu, A., Sugimoto, N., Matsui, I., and Nishizawa, T.: Direct comparison of extinction coefficients derived from Mie-scattering lidar and number concentrations of particles, subjective weather report in Japan, J. Quant. Spectrosc. Radiat. Transf., 153, 77–87, doi:10.1016/j.jqsrt.2014.12.005, 2015.

Shinozuka, Y., and Redemann, J.: Horizontal variability of aerosol optical depth observed during the ARCTAS airborne experiment, Atmos. Chem. Phys., 11, 8489–8495, doi:10.5194/acp-11-8489-2011, 2011.

Smirnov, A., Holben, B.N., Slutsker, I., Giles, D.M., McClain, C.R., Eck, T.F., Sakerin, S.M., Macke, A., Croot, P., Zibordi, G., Quinn, P.K., Sciare, J., Kinne, S., Harvey, M., Smyth, T.J., Piketh, S., Zielinski, T., Proshutinsky, A., Goes, J.I., Nelson, N.B., Larouche, P., Radionov, V.F., Goloub, P., Moorthy, K., Matarrese, R., Robertson, E.J., and Jourdin, F.: Maritime Aerosol Network as a component of Aerosol Robotic Network, J. Geophys. Res., 114, D06204, doi:10.1029/2008JD011257, 2009.

Sugimoto, N., Uno, I., Nishikawa, M., Shimizu, A., Matsui, I., Dong, X., Chen, Y., and Quan, H.: Record heavy Asian dust in Beijing in 2002: Observations and model analysis of recent events, Geophys. Res. Lett., 30, 1640, doi:10.1029/2002GL016349, 2003.

Takemura, T., Nozawa, T., Emori, S., Nakajima, T.Y., and Nakajima, T.: Simulation of climate response to aerosol direct and indirect effects with aerosol transport-radiation model, J. Geophys. Res., 110, D02202, doi:10.1029/2004JD005029, 2005.

van Donkelaar, A., Martin, R.V., Brauer, M., and Boys, B.L.: Use of satellite observations for long-term exposure assessment of global concentrations of fine particulate matter, Environ. Health Perspect., 123, 135–143, doi:10.1289/ehp.1408646, 2015.

Villeneuve, P.J., Weichenthal, S.A., Crouse, D., Miller, A.B., To, T., Martin, R.V., van Donkelaar, A., Wall, C., and Burnett, R.T.: Long-term exposure to fine particulate matter air pollution and mortality among Canadian women, Epidemiology, 26, 4, 536–545, doi:10.1097/EDE.0000000000000294, 2015.